ACS APPLIED POLYMER MATERIALS

pubs.acs.org/acsapm Article

Synergistic Activity of Anticancer Polyphenols Embedded in Amphiphilic Dendrimer Nanoparticles

Shani Ben-Zichri, May Meltzer, Shiran Lacham-Hartman, Sofiya Kolusheva, Uzi Hadad, Niv Papo, and Raz Jelinek*

Cite This: https://doi.org/10.1021/acsapm.2c01316 Read Online

ACCESS | Metrics & More | Article Recommendations | Supporting Information

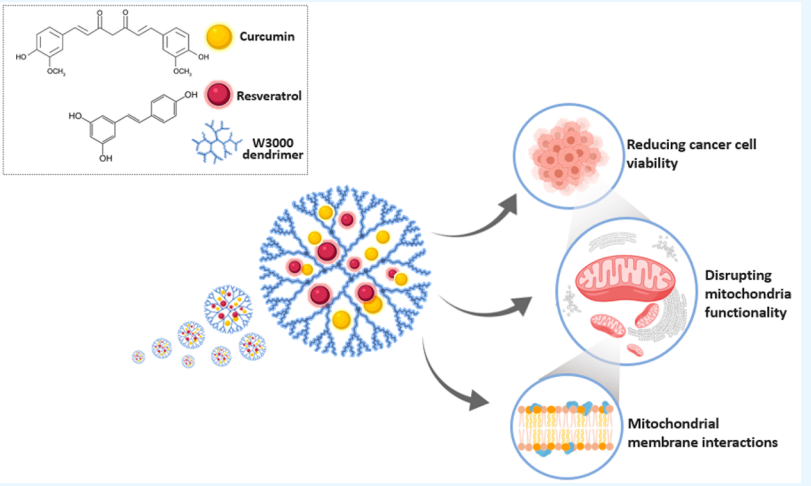

ABSTRACT: Dendritic polymer nanoparticles (NPs) are promising vehicles for drug delivery. Most dendrimer polymer NPs, however, exhibit positive surface charge which make them, in many instances, cytotoxic. We constructed noncationic, amphiphilic dendrimer NPs embedding curcumin and resveratrol, natural polyphenols exhibiting anticancer properties. The curcumin/resveratrol/dendrimer NPs both effectively shielded the embedded polyphenols and facilitated their slow release and, notably, targeted cancer cells. The experimental data trace the cancer cell toxicity of the curcumin/resveratrol/dendrimer NPs to impairment of mitochondrial functions, specifically giving rise to enhanced intracellular calcium release, inhibition of cytochrome *c* oxidase enzyme activity, decreased mitochondrial membrane potential, and mitochondrial membrane perturbation. Importantly, synergism between the dendrimer-NP-embedded curcumin and resveratrol was observed, as more pronounced cancer cell death and mitochondrial disruption were induced by the curcumin/resveratrol/dendrimer NPs as compared to either the freely dissolved polyphenols or amphiphilic dendrimer NPs incorporating curcumin or resveratrol separately. This work suggests that amphiphilic dendrimer NPs encapsulating curcumin and resveratrol may constitute a promising anticancer therapeutic platform.

KEYWORDS: *dendrimer drug carriers, amphiphilic dendrimers, curcumin, resveratrol, mitochondria, cancer*

1. INTRODUCTION

Curcumin and resveratrol are plant-derived polyphenolic compounds reported to exhibit therapeutic properties, including anti-inflammatory, antioxidant, and anticancer activities.[1,2] Curcumin has been shown to inhibit cancer cell proliferation and induced apoptosis in numerous cancer cell types.[3−5] Similar to curcumin, resveratrol also inhibits carcinogenesis.[6,7] Importantly, both curcumin and resveratrol target cancer cells[8,9] and particularly impact cancer cells' mitochondria.[10,11] Previous studies reported that curcumin and resveratrol decrease the mitochondrial membrane potential,[12,13] impair the activity of some mitochondrial respiratory enzymes,[14,15] and trigger mitochondrial outer membrane permeabilization (MOMP).[16,17] Interestingly, curcumin and resveratrol have displayed synergistic effects when administered in tandem.[18,19] Both curcumin and resveratrol, however, are hydrophobic, thus exhibiting low solubility in aqueous solutions and poor bioavailability which hinder their therapeutic applicability. Efforts toward increasing the

Received: July 30, 2022
Accepted: October 25, 2022

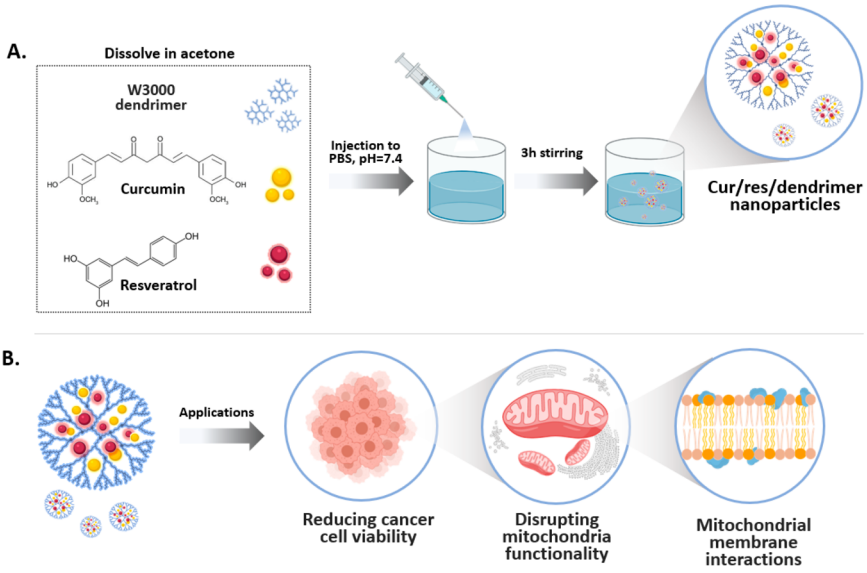

Figure 1. Preparation and anticancer activities of the curcumin/resveratrol/dendrimer nanoparticles. (A) Schematic illustration of the amphiphilic dendrimer NPs encapsulating the curcumin and resveratrol synthesis process. (B) The applications studied.

therapeutic efficacy of curcumin and resveratrol have been accomplished by different methods, particularly their inclusion in varied delivery systems.[20,21]

Dendrimer nanoparticles (NPs) have been investigated as drug delivery carriers.[22−25] In particular, dendrimer NPs have been studied as vehicles for passive and active delivery of anticancer drugs.[26,27] The unique architecture of dendritic (or hyperbranched) polymers furnishes the particles with important functionalities including the nanoscale dimensions, dispersity, stability, and feasibility of diverse functions through chemical surface modifications.[28] The widely used poly(amidoamine) (PAMAM) dendrimers, for instance, display a high density of primary amino surface groups[29] and thus are associated with and efficiently transport DNA into varied cell types.[30,31] However, cationic PAMAM dendrimers exhibit significant toxicity to cells presumably because of their interactions with negative cell surfaces.[32,33] Additionally, the surface amino residues of PAMAM particles might react with carbonyl units in biomolecules, overall limiting their potential therapeutic applicability.

In this study, we synthesized composite NPs comprising an amphiphilic dendritic polymer encapsulating both curcumin and resveratrol. The dendrimer employed (Bolton W3000) is a nonionic and self-emulsifying polymer, comprising hydrophobic unsaturated fatty acid chains and polyethylene glycol (PEG) and forming a dendritic globular structure.[34] This amphiphilic dendrimer was employed in varied applications, for example, as a carrier for the delivery of the chemotherapeutic drug paclitaxel[35] and for separation of aromatic/aliphatic hydrocarbons.[36] Here we show that curcumin/resveratrol/amphiphilic dendrimer NPs had pronounced cytotoxic effects on cancer cells, particularly targeting mitochondria and disrupting mitochondrial functions, including enzyme activities, mitochondrial membrane integrity, and apoptotic effects. Importantly, the biological effects induced by the curcumin/resveratrol/dendrimer NPs were more pronounced than similarly prepared amphiphilic dendrimer NPs comprising the individual polyphenols—curcumin or resveratrol—separately. This synergistic effect may be linked to the enhanced uptake of the polyphenols in the amphiphilic dendrimer matrix and their efficient delivery into the cells. Overall, this study may open innovative avenues for the use of amphiphilic dendrimer NPs as delivery vehicles for naturally extracted anticancer polyphenols.

2. RESULTS AND DISCUSSION

2.1. Preparation and Characterization of the Polyphenol/Dendrimer Nanoparticles. Figure 1A illustrates the preparation scheme of the polyphenol/amphiphilic dendrimer NPs and their tested application at this study (Figure 1B). The composite NPs were synthesized according to the solvent displacement method,[37] in which the amphiphilic dendritic polymer (Bolton W3000) and equimolar concentrations of curcumin and resveratrol were dissolved in acetone and injected into an aqueous buffer solution. Globular NPs were thus formed through the "Ouzo effect" in which nanodroplets are formed without surfactants.[38] A guest molecule loading assay[39] was employed to determine the highest-possible loading of the two compounds within the dendrimer NPs. Hence, different curcumin/resveratrol weight ratios were examined, and the optimal curcumin/resveratrol ratio (both at 0.5 mg per 20 mg of W3000; Figure S1) was determined by use of pertinent calibration curves of curcumin or resveratrol.

Figure 2 depicts bioanalytical characterization of the polyphenol/dendrimer NPs. The representative cryogenic transmission electron microscopy (cryo-TEM) images in Figure 2Ai reveal that incorporation of resveratrol and curcumin within the amphiphilic dendrimer NPs give rise to significant morphological changes. Specifically, while NPs comprising the amphiphilic dendrimer alone appear relatively homogeneous and spherical[40] (Figure 2Ai, left image), the curcumin/resveratrol/dendrimer particles exhibit larger sizes. In addition, the curcumin/resveratrol/dendrimer NPs appear compartmentalized, likely arising from interactions of embedded polyphenols with the dendrimer scaffold. The light-scattering results in Figure 2Aii further attest to the larger sizes of the curcumin/resveratrol/dendrimer NPs (130 ± 9 nm) compared to the bare amphiphilic dendrimer NPs (95 ± 7 nm). Notably, the dimensions of the curcumin/resveratrol/

https://doi.org/10.1021/acsapm.2c01316
ACS Appl. Polym. Mater. XXXX, XXX, XXX−XXX

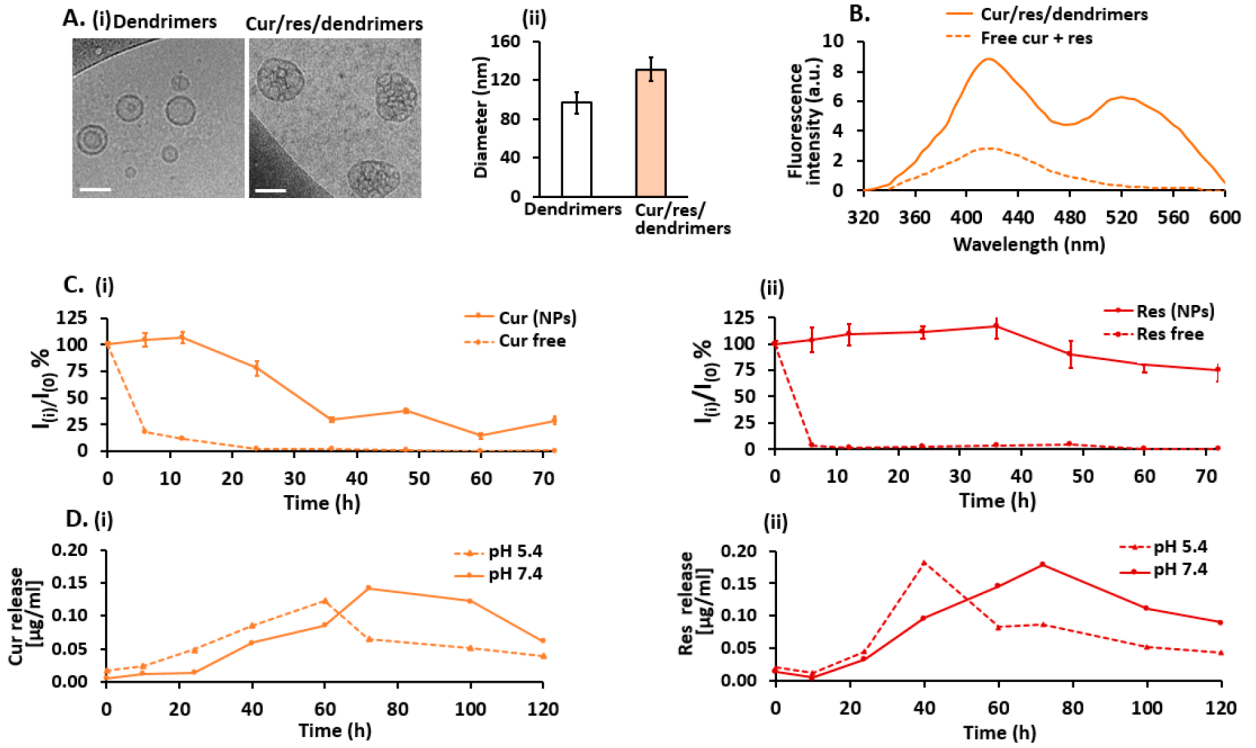

Figure 2. Characterization of the curcumin/resveratrol/dendrimer nanoparticles. (A(i)) Cryo-TEM images of unloaded dendrimer NPs (left image) and curcumin/resveratrol/dendrimer NPs (20:0.5:0.5 mg weight ratio; right). Scale bar corresponds to 100 nm. (ii) Size distribution of the amphiphilic dendrimer NPs (white bar) and cur/res/dendrimers NPs (orange bar), determined by dynamic light scattering. Statistical analysis (n = 3) was performed with an unpaired Student's t test. Results are presented as means (SEM) standard error of three independent replicates. The calculated P values are compared to the control of the experiment. The errors of all results are significant with $P < 0.05$. (B) Fluorescence emission of the curcumin/resveratrol/dendrimer NPs (solid curve) or a free curcumin + resveratrol mixture in buffer (dashed curve). Excitation was at 310 nm (corresponding to resveratrol excitation), and the fluorescence intensity emission values of the highest peak were used for constructing the fluorescence intensity vs time curve (420/520 nm for resveratrol and curcumin, respectively). (C) Light stability assay, in which samples of curcumin/resveratrol/dendrimer NPs, or free curcumin + resveratrol, were exposed to continuous illumination (full spectrum lamp, power 7 W) and fluorescence emission, was monitored over time. The samples were excited at either 450 nm (i) (corresponding to curcumin excitation) or 310 nm (ii) (resveratrol excitation). I_0 indicates the fluorescence emission recorded in t = 0, while I_i accounts for emission of the sample at each time (excitation wavelengths for resveratrol and curcumin were 310 and 450 nm, respectively). (D) Drug release assay. The curcumin/resveratrol/dendrimer NPs were dialyzed in different buffers (pH= 5.4 dashed lines; pH= 7.4 straight lines) for 120 h. The absorbance of curcumin (i) or resveratrol (ii) was measured in each sample (310 and 450 nm for resveratrol and curcumin, respectively), and the release of polyphenols from the dendrimer NPs was determined in μg/mL units by spectrophotometry, through the use of calibration curves for resveratrol and curcumin.

dendrimer NPs, at <200 nm, are in the range of practical drug delivery vehicle applications.[41]

The fluorescence spectroscopy data in Figure 2B further illuminate the proximate nature of curcumin and resveratrol in the amphiphilic dendrimer NPs. When the two polyphenols were freely dissolved in water and excited at 310 nm (resveratrol excitation wavelength[42]), a single small signal at around 420 nm was observed, corresponding to resveratrol emission (Figure 2B, broken spectrum). In comparison, the fluorescence emission spectrum of the curcumin/resveratrol/dendrimer NPs, similarly excited at 310 nm, shows also a pronounced peak at 525 nm, which is the wavelength of curcumin emission[43] (Figure 2B, solid spectrum). This result likely reflects the occurrence of Forster resonance energy transfer (FRET) from the dendrimer-embedded resveratrol to curcumin, indicating the immobilization and proximity between the polyphenols in the dendrimer matrix.

The photolysis experiments in Figure 2C further attest to incorporation of the polyphenols within the dendrimer NPs. Both resveratrol and curcumin are sensitive to photolysis, and exposure to light can lead to degradation and loss of their biological activities.[44,45]Figure 2C depicts the fluorescence emission of the polyphenols (emission wavelengths were at 420 and 520 nm in the case of resveratrol and curcumin, respectively) recorded within 70 h of continuous illumination (utilizing a full spectrum lamp at 7 W power). Notably, the fluorescence emissions of free resveratrol or curcumin in aqueous solutions were almost completely quenched within less than 10 h (Figure 2C, broken lines), reflecting photolysis of the molecules. However, in the case of curcumin/resveratrol/dendrimer NPs, the fluorescence signal recorded for curcumin was retained for more than 35 h (solid line in Figure 2Ci), while resveratrol emission was still significant even after 70 h irradiation (solid line in Figure 2Cii). These results indicate effective shielding of the polyphenols within the dendrimer NPs.

Figure 2D portrays the release profiles of the polyphenols, recorded using the membrane dialysis method, widely employed in nanocarriers' drug release studies.[46] In this assay, the cargo molecules can be easily separated by diffusion through a semipermeable membrane without affecting particle integrity. The release profiles were determined both in pH = 7.4, which mimics the cell cytoplasm conditions, as well as in pH = 5.4, corresponding to the acidic environment in tumor

https://doi.org/10.1021/acsapm.2c01316
ACS Appl. Polym. Mater. XXXX, XXX, XXX−XXX

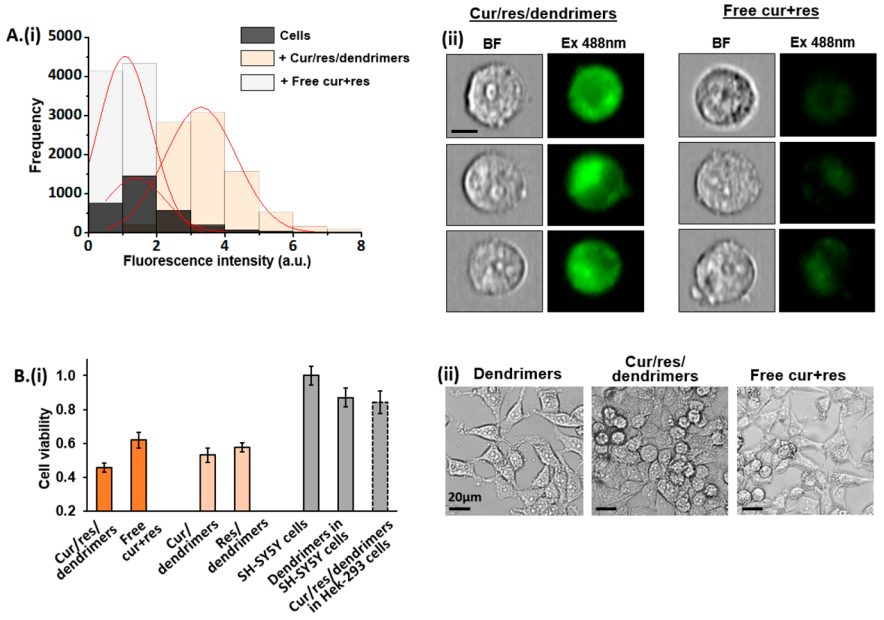

Figure 3. Curcumin/resveratrol/dendrimer nanoparticle cell uptake and inhibition of cancer cells. (A) Flow cytometry histogram quantification (i) and represented images of curcumin/resveratrol/dendrimer NPs or free curcumin + resveratrol uptake by SH-SY5Y cells (ii). The representative images describe the bright-field (BF, left columns) and fluorescence (right columns) images of the cells of each sample (cur/res/dendrimers or free cur + res). The presented fluorescence intensity is according to curcumin Ex (488 nm), and images of the scale bar correspond to 10 μm. (B(i)). Cytotoxicity profile determined by the XTT assay in SH-SY5Y cells. Different samples of NPs (indicated at axis x) incubated with cells for 48 h, followed by addition of the XTT reagent. The control corresponds to nontreated SH-SY5Y cells in which all results are normalized. The final dendrimer concentration was 2.5 mg/mL. Statistical analysis (n = 5) was performed with an unpaired Student's t test. Results are presented as means (SEM) of standard error of five independent replicates. The calculated P values were compared to the control of each experiment. The errors of all results are significant with $P < 0.05$. (ii) Bright-field confocal images of SH-SY5Y cells. Samples were supplemented with bare dendrimer NPs, curcumin/resveratrol/dendrimer NPs, or a free curcumin + resveratrol mixture in buffer. Images were taken after 24 h of incubation of these with the cells. Scale bar corresponds to 20 μm.

cells.[47,48] Importantly, both curcumin and resveratrol were released from the composite NPs earlier in acidic conditions (after 60 and 40 h for curcumin and resveratrol, respectively, Figure 2D). Cancer cells' oxidative metabolism contributes to the acidic microenvironment,[49] and hence the application of nanodelivery systems for payload release accounts for "passive delivery". The early release of curcumin and resveratrol from the NPs testify to their specificity for cancer cells. All together, these results testify that the acidic environment encourages faster release of the polyphenols in less than 3 days.

2.2. Curcumin/Resveratrol/Amphiphilic Dendrimer Nanoparticles Reduce the Viability of Cancer Cells. Figure 3 presents fluorescence and cell viability experiments designed to assess whether the curcumin/resveratrol/dendrimer NPs target and destroy cancer cells. Figure 3Ai depicts histograms accounting for curcumin fluorescence intensity distribution (excitation/emission 488/560 nm[50]) recorded in a flow cytometry experiment following incubation of SH-SY5Y cells, a widely used cancer cell model,[51] for 30 min with either curcumin/resveratrol/dendrimer NPs or with a mixture of freely dissolved polyphenols. The fluorescence emission histograms reveal that significantly higher intensities were recorded following incubation of the cells with the curcumin/resveratrol/dendrimer NPs rather than free polyphenols. The higher fluorescence intensities are ascribed to efficient uptake of curcumin and resveratrol by the SH-SY5Y cells; specifically, we recorded curcumin fluorescence, thereby illuminating polyphenol uptake. While the intrinsic fluorescence of curcumin in solution is low, its incorporation within the hydrophobic environment of the cell membranes gives rise to the pronounced fluorescence intensity, and this may occur due to curcumins lipophilic character.[52,53]

The representative confocal fluorescence microscopy images in Figure 3Aii further attest to the greater uptake of curcumin delivered to the SH-SY5Y cells by the curcumin/resveratrol/dendrimer NPs compared to the free molecule. In the experiment, SH-SY5Y cells were incubated for 30 min with curcumin/resveratrol/dendrimer NPs or free curcumin (curcumin concentration in both cases was 50 μg/mL), and images were recorded (excitation was 488 nm, and the emission detection range was 595−640 nm). Indeed, the curcumin fluorescence in the cells was significantly more intense when the molecule was delivered in the dendrimer NPs compared to cell incubation with free curcumin (Figure 3Aii).

Curcumin and resveratrol are known to target and obliterate cancer cells.[54,55] To evaluate the cell toxicity of the curcumin/resveratrol/dendrimer NPs, we carried out an XTT assay complemented by cell morphology microscopy analysis (Figure 3B). The XTT bar diagram in Figure 3Bi demonstrates that the curcumin/resveratrol/dendrimer NPs (concentration of each polyphenol was 50 μg/mL) decreased the viability of the SH-SY5Y cells by almost 60% after 48 h incubation. This toxic effect was significantly more pronounced compared to free resveratrol and curcumin (i.e., not embedded in dendrimer NPs) that were incubated with the cells at the same concentrations (~40% cell death). In particular, Figure 3Bi further demonstrates a synergistic effect in the case of embedding both curcumin and resveratrol in the dendrimer NPs, as NPs comprising only curcumin or resveratrol (at a concentration of 100 μg/mL) gave rise to less than 50% cell

https://doi.org/10.1021/acsapm.2c01316
ACS Appl. Polym. Mater. XXXX, XXX, XXX−XXX

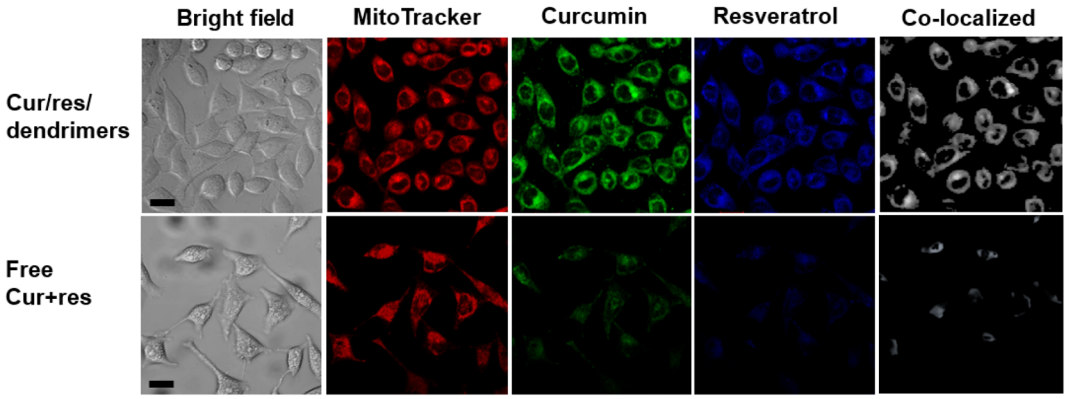

Figure 4. Mitochondria targeting by curcumin/resveratrol/dendrimer nanoparticles in cancer cells. Confocal fluorescence microscopy images of SH-SY5Y cells incubated for 20 min with curcumin/resveratrol/dendrimer NPs (final dendrimer concentration of 2.5 mg/mL; polyphenol concentration was 50 μg/mL) or with a free curcumin + resveratrol mixture (at the same concentration). The cells were then imaged for each fluorophore: MitoTracker Orange (Ex/Em 561/588), curcumin (Ex/Em 488/561), and resveratrol (Ex/Em 405/488). Colocalized images were obtained by analysis with Image J software. Scale bar corresponds to 20 μm.

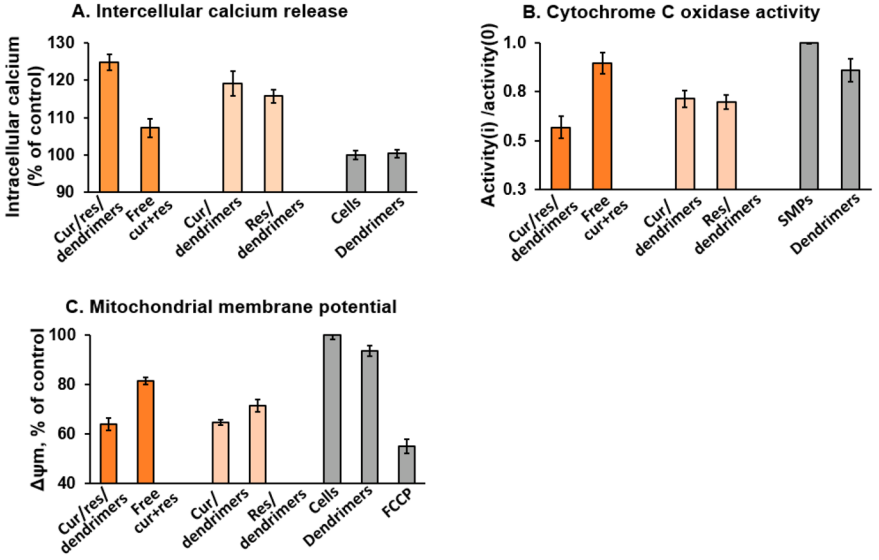

Figure 5. Disruption of mitochondrial functionalities induced by curcumin/resveratrol/dendrimer NPs. (A) Intercellular calcium release assay. SH-SY5Y cells were incubated with different NP samples (indicated at the *x* axis). The samples were incubated for 48 h followed by determination of calcium levels using the Fluo-4 direct assay kit. (B) Cytochrome *c* oxidase (COX) activity. SMPs derived from SH-SY5Y cells were treated with different samples (indicated at the *x* axis). COX absorbance at 550 nm was measured in the presence of a ferrocytochrome *c* solution (0.22 mM). The *y* axis corresponds to the COX enzyme activity ratio, in which activity(i) represents the enzyme activity measured in SMP + sample and activity(0) is the enzyme activity in SMPs alone. Results are presented as means ± standard error of the mean (SEM) of five replicates. (C) Mitochondrial membrane potential depolarization in SH-SY5Y cells. The cells were incubated with different samples (indicated at the *x* axis) for 24 h, after which the TMRE mitochondrial membrane potential assay was performed. Carbonyl cyanide *p*-trifluoromethoxyphenylhydrazone (FCCP) served as the positive control for depolarization of the mitochondrial membrane potential. The *y* axis depicts the mitochondrial membrane potential ($\Delta\Psi$m). Statistical analysis (n = 5) was performed with an unpaired Student's *t* test. Results are presented as mean (SEM) standard error of five independent replicates. The calculated *P* values are compared to the control of each experiment. The errors of all results are significant with $P < 0.05$.

death. Notably, significantly less toxicity was observed when the curcumin/resveratrol/dendrimer NPs were incubated with normal (noncancerous) Hek-293 cells (around 20% cell death, Figure 3Bi, rightmost bar), underscoring targeting of cancer cells by the polyphenol/dendrimer NP system.

The microscopy images in Figure 3Bii complement the XTT assay results, furnishing visual evidence for the cytotoxic effect of the curcumin/resveratrol/dendrimer NPs on cancer cells. Specifically, addition of the curcumin/resveratrol/dendrimer NPs (concentration of each polyphenol was 50 μg/mL) to the SH-SY5Y cancer cells gave rise to formation of cell rounding and shrinking, both reflecting typical apoptotic effects on cells (Figure 3Bii). In comparison, and echoing the XTT data, addition of a curcumin + resveratrol mixture not sequestered in NPs (concentration of each polyphenol was 50 μg/mL) resulted in lesser apoptotic effects, displaying higher abundance of cells exhibiting normal shapes (Figure 3Bii).

2.3. Targeting Mitochondria in Cancer Cells by Curcumin/Resveratrol/Dendrimer Nanoparticles. Anticancer polyphenols such as curcumin and resveratrol specifically inhibit mitochondria respiratory activities and induce apoptosis.[56−59] The confocal fluorescence microscopy

https://doi.org/10.1021/acsapm.2c01316
ACS Appl. Polym. Mater. XXXX, XXX, XXX−XXX

images in Figure 4 examine mitochondrial targeting by the curcumin/resveratrol/dendrimer NPs in SH-SY5Y cancer cells. In the experiments, cells stained with the mitochondria-specific fluorescent dye MitoTracker Orange were coincubated with curcumin/resveratrol/dendrimer NPs or with the free curcumin and resveratrol mixture (at the same polyphenol concentrations). The cells were then imaged in blue (Ex/Em 405/488 nm, depicting resveratrol fluorescence), green (Ex/Em 488/561 nm, illuminating curcumin uptake), or red (Ex/Em 561/566 nm, showing the fluorescence of MitoTracker Orange).

As shown in Figure 4 (top row), following incubation of the SH-SY5Y cells with the curcumin/resveratrol/dendrimer NPs, colocalization of both resveratrol and curcumin with MitoTracker Orange was apparent, indicating delivery of the polyphenols to the mitochondria. In contrast, when the SH-SY5Y cells were incubated with curcumin and resveratrol that were not NP-embedded, much lower mitochondria uptake was observed (Figure 4, bottom row). Overall, the fluorescence confocal microscopy data in Figure 4 furnish evidence for targeted mitochondria delivery of curcumin and resveratrol via the amphiphilic dendrimer NPs. Additional quantitative colocalization analysis is presented in Figure S3.

We investigated the effects of the curcumin/resveratrol/dendrimer NPs on mitochondrial functionalities, in comparison with polyphenols freely dissolved in solution as well as compared to amphiphilic dendrimer NPs encapsulating only curcumin or resveratrol (Figure 5). Figure 5A depicts intracellular calcium levels measured in SH-SY5Y cells following incubation with curcumin/resveratrol/dendrimer NPs (concentration of each compound was 50 μg/mL), a freely dissolved curcumin and resveratrol mixture (at the same concentrations as in the NPs), or dendrimer NPs comprising only resveratrol or curcumin (concentration of each was 100 μg/mL). Intracellular calcium is an important parameter for regulating mitochondrial function and adenosine triphosphate (ATP) production.[60,61] Impairment of the outer mitochondrial membrane might lead to release of mitochondrially associated Ca^{2+} and a concomitant increase in intracellular calcium levels.[62,63] Previous studies reported that both curcumin and resveratrol induced intracellular calcium release in cancer cell lines.[64,65] The bar diagram in Figure 5A shows that the curcumin/resveratrol/dendrimer NPs induced more than 25% higher intracellular calcium release in SH-SY5Y cells compared to untreated cells. The corresponding intracellular calcium release when a mixture of freely dissolved curcumin and resveratrol was added to the SH-SY5Y cells was less than 10%, attesting to the greater disruption of mitochondrial function mediated by the curcumin/resveratrol/dendrimer NPs. Furthermore, incubation of the SH-SY5Y cells with curcumin/dendrimer NPs or with resveratrol/dendrimer NPs induced lesser Ca^{2+} release (19% and 15%, respectively) than curcumin/resveratrol/dendrimer NPs, attesting to a synergistic effect when the two polyphenols were embedded together in the amphiphilic dendrimer NPs.

Figure 5B presents the effects of the polyphenols on the enzymatic activity of cytochrome *c* oxidase (COX). COX is a prominent mitochondrial respiratory enzyme, playing a key role in energy generation.[66] Previous reports demonstrated modulation of COX activity by curcumin or resveratrol.[67,68] In the experiments depicted in Figure 5B, we extracted mitochondria from SH-SY5Y cells and constructed "inside-out" submitochondrial particles (SMPs).[69] SMPs allow monitoring of COX activity since they expose to solution the inner mitochondrial membrane and associated membrane proteins, such as COX. Control experiments confirmed inversion of the inner mitochondrial membrane in the SMPs while retaining membrane functionality (Figure S2). Echoing the intracellular calcium release analysis in Figure 5A, and Figure 5B demonstrates significant attenuation of COX activity following incubation of the SMPs extracted from the SH-SY5Y cells with curcumin/resveratrol/dendrimer NPs (activity ratio 0.56 $\pm$ 0.07). Furthermore, COX inhibitory activity was less pronounced when the SMPs were incubated with the NP-free curcumin and resveratrol mixture (0.89 $\pm$ 0.09). Importantly, lesser COX inhibition was recorded when amphiphilic dendrimer NPs comprising either curcumin or resveratrol individually were added to the SMPs (0.71 $\pm$ 0.06 and 0.69 $\pm$ 0.03, respectively), attesting to a synergistic biological effect when the two polyphenols were embedded together in the dendrimer NPs, echoing the calcium release experimental results in Figure 5A.

Figure 5C presents mitochondrial membrane potential quantification, further attesting to the significant disruption of mitochondrial functions by the curcumin/resveratrol/dendrimer NPs. Mitochondrial membrane potential is an important mitochondrial activity marker.[70] Depolarization of mitochondrial membrane potential may lead to bioenergetic stress, resulting in release of apoptotic factors, leading to cell death.[70] In the experiments outlined in Figure 5C, the membrane potential of SMPs extracted from SH-SY5Y cells was determined by the tetramethylrhodamine ethyl ester perchlorate (TMRE) assay. TMRE is a cell-permeable, positively charged dye, accumulating in active mitochondria.[71] Corroborating the calcium release and COX inhibition experiments, Figure 5C demonstrates that significant membrane depolarization (around 40%) was induced upon incubation of the SMPs with the curcumin/resveratrol/dendrimer NPs, while the free curcumin/resveratrol mixture in solution induced significantly lower, ~20%, membrane depolarization. Cyanide *p*-trifluoromethoxyphenylhydrazone (FCCP) served as a positive control for mitochondrial membrane depolarization. The data in Figure 5 are consistent with the cell viability (Figure 3) and mitochondria targeting experiments (Figure 4), attesting to the pronounced anticancer effects of the curcumin/resveratrol/dendrimer NPs. Additional experiments inspecting the impact of curcumin/resveratrol/dendrimer NPs on mitochondria functionality of noncancerous Hek-293 cells indicate lesser mitochondrial disruption (Figure S4), attesting to cancer cell targeting by the amphiphilic NPs.

An important result underscored in the data depicted in Figures 3−5 is the apparent synergistic effect when curcumin and resveratrol are delivered together in the amphiphilic dendrimer NPs. Previous studies have reported that administration of curcumin and resveratrol in tandem resulted in synergistic anticancer effects *in vitro* and *in vivo* in varied human tumor cells.[18,72] In particular, curcumin and resveratrol were shown to more effectively stimulate apoptotic mitochondrial enzymes when delivered together to cancer cells[73] and gave rise to a synergistic antiproliferative effect.[74] This effect was ascribed to attenuation of antiapoptotic proteins and activation of growth factor receptors, leading to higher activity when both molecules were furnished.[75] Previous studies indicated that resveratrol may stabilize curcumin, and this enhanced chemical stability could increase the biological efficacy of both molecules, for example, through inhibition of

https://doi.org/10.1021/acsapm.2c01316
ACS Appl. Polym. Mater. XXXX, XXX, XXX−XXX

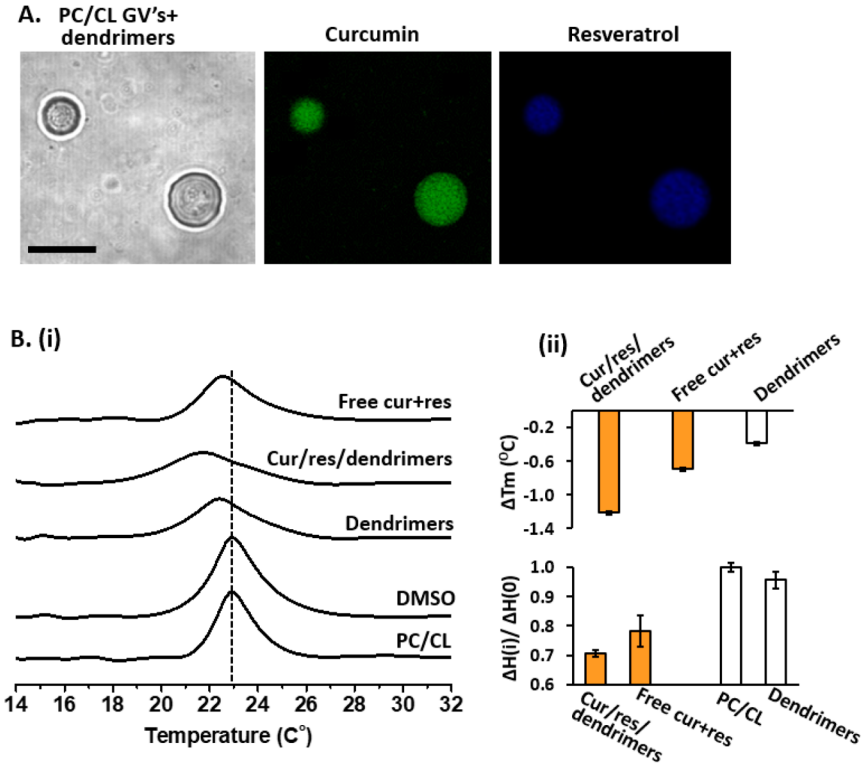

Figure 6. Membrane interactions of the curcumin/resveratrol/dendrimer nanoparticles. (A) Confocal fluorescence microscopy of DOPC/CL GVs (9:1 mol ratio between DOPC and CL) incubated with curcumin/resveratrol/dendrimer NPs (1 μg/mL final concentration of the dendrimers). Bright field (left image), excitation/emission of 488 nm/561−588 nm for curcumin (middle image), and excitation/emission of 405 nm/488−561 nm for resveratrol. Scale bars correspond to 10 μm. (B) Differential scanning calorimetry (DSC) thermogram (i) and thermodynamic parameters (ii) obtained in DMPC/CL MLVs (98:2 mol ratio, 1 mM) were supplemented with the following: bare dendrimer NPs (dendrimers), curcumin/resveratrol/dendrimer NPs, or the free curcumin + resveratrol mix. The samples of DMPC/CL MLVs alone (PC/CL) or MLVs mixed with DMSO were used as the control. DSC parameters recorded for the multilamellar vesicle suspensions are indicated in (B(ii)) as follows: ΔTm, the difference between phase transition temperatures recorded upon addition of NP samples and control MLVs, and $\Delta H(i)/\Delta H(0)$, the enthalpy ratio in which $\Delta H(i)$ corresponds to the enthalpy change after sample addition and $\Delta H0$ is the control vesicle sample. Statistical analysis (n = 3) was performed with an unpaired Student's t test. Results are presented as mean (SEM) standard error of three independent replicates. The calculated P values are compared to the control of each experiment. The errors of all results are significant with $P < 0.05$.

NF-κB activity in colon tumor cells and concomitant stimulation of apoptosis.[76] Other *in vivo* studies demonstrated that when the two polyphenols were provided together apoptotic pathways were induced through downregulation of Bcl-2 and upregulation of Bax and cytosolic release of cytochrome *c*.[18]

To complement the mitochondria functional analyses in Figure 5, we additionally investigated the effects of the curcumin/resveratrol/dendrimer NPs upon the physicochemical properties of mitochondrial membranes, as membrane bilayers constitute likely sites for docking and uptake of the lipophilic polyphenols[77] (Figure 6). Figure 6A examines incorporation of resveratrol and curcumin within giant vesicles (GVs) comprising dioleylphosphatydilcholine (DOPC) and cardiolipin (CL) (98:2 mol ratio), mimicking mitochondrial outer membrane composition.[78] GVs are useful models for cellular membranes in light of their dimensions and low curvatures.[79]Figure 6A reveals efficient uptake of curcumin and resveratrol by the GVs. Notably, significant fluorescence intensities of resveratrol or curcumin were apparent when the vesicles were incubated with curcumin/resveratrol/dendrimer NPs (Figure 6A), accounting for the effective delivery of the polyphenols by the amphiphilic dendrimer NPs.

Figure 6B depicts differential scanning calorimetry (DSC) measurements in which DMPC/CL (98:2 mol ratio) vesicles were employed as mitochondrial membrane mimics.[78] DSC permits assessing the effect of membrane-active substances upon bilayer thermodynamic parameters.[80]Figure 6B shows that the curcumin/resveratrol/dendrimer NPs had a significant effect on membrane bilayer properties. Specifically, the polyphenol/dendrimer NPs reduced the gel−liquid phase transition temperature by an experimentally significant 1.2 °C (thermogram peak shift shown in Figure 6Bi and shown quantitatively in Figure 6Bii), ascribed to misalignment of the lipids' acyl tails due to greater bilayer disorder. Furthermore, the effect of the curcumin/resveratrol/dendrimer NPs upon ΔTm of the DMPC/CL vesicles was significantly more pronounced than addition of the free polyphenols, which may account for the more effective mitochondria targeting by the polyphenol/dendrimer NPs (e.g., Figures 3−5).

The DSC data in Figure 6Bii further reveal a significant decrease of the enthalpy change ratio (ΔHi/$\Delta H0$) induced by the curcumin/resveratrol/dendrimer NPs (0.71 ± 0.01). The lower enthalpy ratio indicates less pronounced participation of the bilayer lipids in the phase transition, ascribed to interactions of the polyphenol dendrimer NPs which disengage the lipid molecules. Notably, the enthalpy change ratio induced by the curcumin/resveratrol/dendrimer NPs was lower than value calculated for the vesicles following incubation with the free curcumin + resveratrol mixture (0.79 ± 0.05, Figure 6Bii),

https://doi.org/10.1021/acsapm.2c01316
ACS Appl. Polym. Mater. XXXX, XXX, XXX−XXX

reflecting a lesser impact of the free polyphenols on the bilayer membrane.

Together, the fluorescence microscopy and DSC results in Figure 6 attest to affinity and perturbation of mitochondria-mimic membrane bilayers by curcumin and resveratrol delivered via the amphiphilic dendrimer NPs. Curcumin and resveratrol are lipophilic and are known to accumulate in cell membranes.[81,82] In addition, previous studies have shown that these polyphenols induced lysis of mitochondrial membranes in several cancer cells.[59,83−85] As such, membrane localization and bilayer interactions may contribute to the effects of curcumin and resveratrol upon membrane protein functionalities, such as the disruption of COX activity or elevated intracellular calcium levels (Figure 5). Indeed, increased intracellular calcium levels, induced by permeability transition pores (PTPs) in the inner mitochondrial membrane, lead to cell apoptosis.[86] This factor may contribute to the adverse impact of the NPs upon mitochondria in cancer cells and specifically mitochondrial membranes; therefore, its inhibition may account for uptake of the curcumin/resveratrol/dendrimer NPs by the mitochondrial membrane, providing a possible mechanistic pathway for its functional disruption.

3. CONCLUSIONS

In conclusion, this study describes codelivery of curcumin and resveratrol to cancer cells via incorporation within an amphiphilic dendrimer NP. Cancer cell viability data reveal significant cytotoxicity of the curcumin/resveratrol/dendrimer NPs upon incubation with the cells. Functional mitochondria assays demonstrated that the polyphenol/dendrimer NPs interact with the mitochondrial membrane, affecting intracellular calcium release, impairment of COX activity, and lower mitochondrial membrane potential. Importantly, the effects of the curcumin/resveratrol/dendrimer NPs were more pronounced compared to dendrimers hosting curcumin or resveratrol individually. Overall, this study may point to amphiphilic dendrimers as a possible therapeutic vehicle against cancer.

4. EXPERIMENTAL SECTION

4.1. Materials. The hyperbranched polyester Bolton W3000 was purchased from Polymer Factory (Stockholm, Sweden). 3,4′,5-Trihydroxy-*trans*-stilbene (resveratrol) was obtained from Glentham Life Sciences (Wiltshire, UK). (*E*,*E*)-1,7-Bis(4-hydroxy-3-methoxyphenyl)-1,6-heptadiene-3,5-dione (curcumin), cytochrome *c* (equine heart), cytochrome *c* oxidase (bovine heart), and DL-dithiothreitol (DTT) were purchased from Sigma-Aldrich (Rehovot, Israel). Cardiolipin (Heart, Bovine) sodium salt (CL), 1,2-dioleoyl-*sn*-glycero-3-phosphocholine (DOPC) and 1,2-dimyristoyl-*sn*-glycero-3-phosphocholine (DMPC) were purchased from Avanti Polar Lipids Inc. (AL, USA). A calcium fluorometric assay kit was obtained from Biovision (CA, USA), and a cell proliferation kit (XTT based) and Dulbecco's phosphate-buffered saline (DPBS) without calcium and magnesium were obtained from Biological Industries (Beit Haemek, Israel). The TMRE mitochondrial membrane potential assay kit was purchased from Abcam (Cambridge, UK).

4.2. Preparation of Dendrimer Nanoparticles. Curcumin/resveratrol/dendrimer NP synthesis was prepared by the solvent displacement method.[87] Briefly, 20 mg of Bolton W3000 dendrimer was interspersed with 0.5 mg of curcumin and 0.5 mg of resveratrol, each dissolved in 1 mL of acetone. The solutions were mixed and injected slowly into a magnetically stirred solution containing 10 mL of DPBS buffer (pH = 7.4) by a syringe needle submerged within the aqueous solution and pressed against the glass beaker wall. The resulting suspension was stirred for 3 h in a fume hood to allow removal of residual acetone. The solutions were further centrifuged at 4000 rpm for 10 min to discard remnant curcumin and resveratrol and kept at 4 °C after preparation. As control samples, curcumin or resveratrol individually (1.0 mg each) was used to prepare curcumin/dendrimer or resveratrol/dendrimer NPs (W3000/polyphenol weight ratio was 20:1 mg). For the light stability assay (described below), free curcumin or resveratrol NPs were prepared, and 5 mg of sample from each polyphenol was dissolved in acetone and injected into DPBS buffer according to the procedure described here for the formation of NPs.

4.3. Cell Cultures. Neuroblastoma (SH-SY5Y) and human embryo kidney (Hek-293) cell lines were grown in Dulbecco's modified Eagle medium (DMEM) at 37 °C and 5% CO_2 atmosphere conditions. The cells were supplemented with 10% tetracycline-free fetal bovine serum (FBS), L-glutamine (2 mM), and penicillin (100 units/ml)/streptomycin (0.1 mg/mL) (Gibco, Israel).

4.4. Mitochondria Isolation and Submitochondrial Particle (SMP) Preparation. The mitochondria isolation and SMP preparation were performed according to an established protocol accomplished in our previews study.[88] Briefly, SH-SY5Y cells were harvested at 75−80% confluence and mixed with hypotonic solution followed by incubation of the cells for 10 min on ice according to a protocol published earlier.[89] Portions from the cell's suspension were homogenized with a Teflon glass homogenizer and diluted with hypertonic solution. The cell aliquots were then diluted with isolation buffer followed by a series of ultracentrifugations for mitochondria isolation. The final mitochondria pellet was suspended in MiR06 buffer and stored at −80 °C until use.

Submitochondrial particles (SMPs) were prepared according to published protocols.[90] Isolated mitochondria extracted from SH-SY5Y cells were diluted with sonication buffer. The mitochondria suspension was then probe-sonicated in order to form an inside-out oriented SMP (in which the inner mitochondrial membrane is facing out to the medium solution). The SMP protein concentrations (μg of protein/mL) were determined by the Bradford test.

4.5. Preparation of Giant Lipid Vesicles (GVs). GVs were prepared through a rapid evaporation method.[91] GVs comprising DOPC/CL (90:10) lipid compositions were dissolved in 1 mL of chloroform in a 250 mL round-bottom glass flask. A volume of 5 mL of Tris buffer (10 mM, pH = 7.4) containing sucrose (0.3 M) was carefully added with a pipet to the flask wall. The chloroform solvent was subsequently removed in a rotary evaporator under reduced pressure conditions at room temperature. After evaporation for 4−5 min, the resulting vesicle solution exhibited a turbid appearance and was used on the day of preparation.

4.6. Cryogenic Transmission Electron Microscopy. Solutions of bare dendrimer NPs (dendrimer final concentration was 20 mg/mL) or dendrimers with curcumin and resveratrol (0.5 mg/mL each) were prepared as described above. A 3 μL droplet from each sample was deposited on a glow-discharged TEM grid (300 mesh Cu lacey substrate grid; Ted Pella). The excess liquid was blotted with a filter paper, and the specimen was rapidly plunged into liquid ethane precooled with liquid nitrogen in a controlled environment (Leica EM GP). The vitrified samples were transferred to a cryo-specimen holder and examined at −180 °C using an FEI Tecnai 12 G2 TWIN TEM operated at 120 kV in low-dose mode. The TEM images were obtained with a Gatan charge-coupled device camera (model 794).

4.7. Dynamic Light Scattering (DLS). Dynamic light-scattering measurements were performed on bare dendrimer NPs (W3000) or dendrimer NPs comprising curcumin and resveratrol, and the final dendrimer concentration was 100 μg/mL. The procedure was performed by Malvern nano zetasizer (Malvern, UK) using a laser source of λ = 633 nm wavelength and a detector at a scattering angle of θ = 173°. The hydrodynamic diameters of the samples were then immediately measured by DLS. The samples were measured in a disposable cuvette and kept at room temperature during the analysis. For each sample, DLS data were recorded three times with 10−15 sub runs using the multimodal mode. The *Z*-average diameter (nm) was calculated from the correlation function using Malvern technology

https://doi.org/10.1021/acsapm.2c01316
ACS Appl. Polym. Mater. XXXX, XXX, XXX−XXX

software. Experiments were repeated three times to verify the reproducibility

4.8. Curcumin and Resveratrol Fluorescence. The fluorescence of curcumin or resveratrol was measured in dendrimer NPs prepared by the protocol described above. An aliquot of curcumin/resveratrol/dendrimer NP solution (polyphenol concentrations were 5 μg/mL each, and the final dendrimer concentration was 200 ug/mL) or the same concentrations of free curcumin and resveratrol (5 μg/mL each) were dissolved in DMSO, supplemented with 1 mL of DPBS buffer (pH = 7.4). Fluorescence was measured on the Fluorolog spectrofluorimeter device (HORIBA, Japan) using an excitation wavelength of 310 nm and emission range of 330−600 nm.

4.9. Light Stability. The fluorescence emission of curcumin or resveratrol embedded in the dendrimer NPs was examined after exposure to continuous light illumination. Curcumin/resveratrol/dendrimer (0.5:0.5:20 mg) or free polyphenol NPs (concentration of each was 0.5 mg/mL) serving as the control were exposed to continuous illumination by a bulb lamp (7 W) for a duration of 70 h. An aliquot of each sample was examined in intervals of 5−10 h, and the fluorescence emission of curcumin (exc. wavelength 450 nm) or resveratrol (exc. wavelength 310 nm) was recorded by a Fluorolog spectrofluorimeter (HORIBA, Japan). The maximal fluorescence values of each sample ($I_{(i)}$) were normalized according to the maximal fluorescence emission at t = 0 h ($I_{(0)}$) to determine the percentage of $I_{(i)}/I_{(0)}$ ratio.

4.10. Curcumin and Resveratrol Release from the Dendrimer NPs. Polyphenol release from the curcumin/resveratrol/dendrimer NPs was evaluated using a dialysis bag diffusion technique.[92] Briefly, 5 mL of curcumin/resveratrol/dendrimer NP suspension (0.5:0.5:20 mg, respectively) was inserted into a dialysis membrane (regenerated cellulose; MWCO 10K). Dialysis was performed using 50 mL of DPBS buffer (pH = 7.4) with 10% ethanol to enable enhanced release for the poorly water-soluble curcumin or resveratrol. The assay was performed by gentle shaking at 37 °C. At predetermined time intervals (∼ every 10−20 h) for a duration of 240 h, 1 mL aliquots of the aqueous solution were withdrawn from the release medium and replaced with fresh medium. The samples were then extracted in chloroform and dried under evaporation conditions followed by redissolving the dry sample in 1 mL of ethanol. The amount of curcumin or resveratrol released in each time interval was determined by UV−vis spectroscopy at 310 nm (for resveratrol) and 430 nm (for curcumin) according to the calibration curve of curcumin or resveratrol. The concentrations were in μg/mL.

4.11. Imaging Flow Cytometry. SH-SY5Y cells were treated with curcumin/resveratrol/dendrimer NPs (dendrimer final concentration was 2.5 mg/mL) or a respective amount of free curcumin or resveratrol (50 μg/mL each) and incubated with the cells for 30 min. Cells were then harvested, centrifuged at 1200 rpm for 5 min, and rinsed with 500 μL of DPBS. Aliquots of each cell sample were analyzed by an Amnis Image StreamX MK II imaging flow cytometer (Seattle, WA), acquiring 1000 images of cells on average in the bright-field channel and the fluorescence emission channel using an excitation laser operating at 488 nm with 10 mW power (emission detection in 595−640 nm; objective 60NA 0.75). Histogram analysis was carried out using Amnis IDEAS software.

4.12. Cell Viability Assay. The effect of the curcumin/resveratrol/dendrimer NPs on SH-SY5Y cells was assayed by an XTT-based kit (Biological Industries) according to the manufacturer protocol. Cells were seeded on a 96-well plate (1×10^4 cells per well) coated for tissue culture (Costar) and incubated at 37 °C and 5% CO_2 conditions for 24 h. The medium was then replaced with fresh Dulbecco's modified Eagle medium (DMEM) supplemented with 10% fetal bovine serum (FBS), L-glutamine (2 mM), and penicillin (100 units/mL)/streptomycin (0.1 mg/mL). The cells were treated with bare dendrimer NPs, curcumin/resveratrol/dendrimer NPs, dendrimers that contain curcumin or resveratrol separately (curcumin/dendrimers or resveratrol/dendrimers), or free curcumin or resveratrol at the corresponding concentrations. The final dendrimer concentration in all experiments was 2.5 mg/mL and 50 μg/mL for both curcumin and resveratrol. The sample solutions were further incubated for 48 h at 37 °C/5% CO_2. Finally, 50 μL of the XTT reagent was added to each well, and the viable cells were measured at 490 nm with 5 repeats on a BioTek Synergy 4 microplate reader (Winooski, VT, USA). Data analysis was performed by normalizing each sample result according to the cell-only control.

4.13. Confocal Microscopy. SH-SY5Y cells were seeded on 0.8 cm^2 microslides (Nunc Lab-Tek, ThermoFisher Scientific, USA) at a density of 1×10^4 cells per well and maintained overnight. For bright-field measurements, cells were treated with bare dendrimer NPs, curcumin/resveratrol/dendrimer NPs (final polyphenol concentrations were 50 μg/mL, and the dendrimer concentration was 2.5 mg/mL), or pertinent concentrations of free curcumin or resveratrol dissolved at DMSO. All samples were incubated for 24 h, and bright-field images were recorded after preset timeframes. For fluorescence imaging, cells were incubated with curcumin/resveratrol/dendrimer NPs or an adapted amount of free curcumin or resveratrol dissolved in DMSO. All samples were dissolved in the growth medium for 20 min at 37 °C and then rinsed with DPBS subsequently, and the final polyphenol concentrations were 50 μg/mL. Cells were then stained with 20 nM MitoTracker Orange CM Ros for an additional 30 min at 37 °C. Images were acquired on a Zeiss LSM880 confocal microscope (Jena, Germany), using a CLSM plan-Aprochromat, ×20/0.8 M27 objective. Excitation wavelengths of curcumin, resveratrol, or MitoTracker Orange were 405/448/561 nm, respectively. For fluorescence imaging of GVs, samples of bare dendrimers or curcumin/resveratrol/dendrimer NPs (final polyphenols concentrations 50 μg/mL) were supplemented with 1 mM DOPC/CL (90:10) GV solution. Images were acquired on a Zeiss LSM880 confocal microscope (Jena, Germany), using the CLSM plan-Aprochromat, ×20/0.8 M27 objective. Excitation wavelengths of curcumin or resveratrol were 405/448 nm, respectively

4.14. Intracellular Calcium Release. The intracellular calcium levels measured by seeding 1×10^4 of SH-SY5Y cells per well, in a black-clear bottom 96-well plate. Cells were treated with bare dendrimer NPs, curcumin/resveratrol/dendrimer NPs, curcumin/dendrimers or resveratrol/dendrimers NPs, or a free curcumin and resveratrol mixture for 48 h. The final dendrimer concentration was 2.5 mg/mL. The cells were subjected to the intracellular calcium assay using the Flou-4-direct calcium assay kit (Biovision), according to the manufacturer protocol, which measures the increase in fluorescence relative to nontreated control. Changes of the fluorescence emission were measured by a BioTek Synergy 4 microplate reader (Winooski, VT, USA) with fluorescence excitation and emission wavelengths of 494 and 516 nm, respectively.

4.15. Cytochrome *c* Oxidase (COX) Activity. COX activity was performed according to established protocols measured in an earlier study.[88] Briefly, the decrease in absorbance was monitored at 550 nm of reduced ferrocytochrome *c* solution in the presence of SMPs (preparation protocol of the SMPs as outlined above). Samples of SMPs derived from SH-SY5Y cells (200 μg/mL final concentration) were mixed with dendrimer NPs, curcumin/resveratrol/dendrimer NPs, curcumin/dendrimers, resveratrol/dendrimer NPs, or a free curcumin + resveratrol mixture. The ratio between the SMP/dendrimer NPs was 1:1 (w/w). Each sample was supplemented with enzyme buffer (10 mM Tris HCl, 250 mM sucrose, pH = 7.0) to complete the total reaction volume to 1.1 mL. To initiate the oxidation reaction between ferricytochrome *c* and COX, 50 μL of ferrocytochrome *c* substrate was added to the enzyme. Amounts of 200 μL aliquots were measured five times using a 96-well plate. The kinetic changes of absorbance were measured for 20 min, with 20 s intervals at 25 °C on a BioTek Synergy 4 microplate reader (Winooski, VT, USA). The activity of COX (units/mL) was calculated according to the equation:

$$\text{COX activity}\left(\frac{\text{units}}{\text{mL}}\right) = \frac{\Delta A/\text{s} \times \text{dil} \times V(t)}{V(s) \times 21.84} \quad (1)$$

in which ΔA/s represents the reaction rate of a sample subtracted from blank; dil refers to the dilution factor of ferrocytochrome *c*

https://doi.org/10.1021/acsapm.2c01316
ACS Appl. Polym. Mater. XXXX, XXX, XXX−XXX

solution; $V(t)$ is total reaction volume; $V(s)$ is the volume of ferrocytochrome c substrate added to initiate oxidation; and 21.84 is the extinction coefficient between ferrocytochrome c and ferricytochrome c at 550 nm.[93] Unit definition: One unit oxidizes 1.0 μmol of ferrocytochrome c per second at pH = 7.0 and 25 °C.

4.16. Mitochondrial Membrane Potential Assay. For measuring mitochondrial membrane potential depolarization, 1×10^4 SH-SY5Y cells were seeded in each well in a black-clear bottom 96-well plate. Cells were treated with preformed 2.5 mg/mL dendrimer NPs, curcumin/resveratrol/dendrimer NPs, curcumin/dendrimers or resveratrol/dendrimers, or a free curcumin + resveratrol mixture (50 μg/mL each) for 24 h. Cells were subjected by the tetramethylrhodamine ethyl ester perchlorate (TMRE) mitochondrial membrane potential assay kit (Abcam, Cambridge, MA) according to the manufacturer's protocol, which measures the reduction in fluorescence relative to an untreated control. The fluorescence measurements were acquired by using a Synergy2 microplate spectrophotometer (BioTek) with fluorescence excitation and emission wavelengths of 549 and 575 nm, respectively. The addition of carbonyl cyanide-*p*-trifluoromethoxy phenylhydrazone (FCCP) at 20 μM to the cells served as a positive control, inducing complete depolarization of the mitochondrial membrane potential.

4.17. Differential Scanning Calorimetry (DSC) Assay. Non-sonicated multilamellar vesicles (MLVs) at 1 mM total lipid concentration were prepared by dissolving a DMPC/CL (98:2) dry lipid mixture in 4 mL of Dulbecco's phosphate-buffered saline (pH = 7.4). Glass beads were then added to the suspension, and the sample was thoroughly dispersed for 30 min at 30 °C until a homogeneous solution was obtained. The DSC experiments were performed on a VP-DSC microcalorimeter (MicroCal, Northampton, MA, USA). Dendrimer NPs (2.5 mg/mL), curcumin/resveratrol/dendrimer NPs, and a free curcumin + resveratrol mixture (50 μg/mL each) were added to the MLVs, and heating scans were recorded at a rate of 60 °C/h. The data analysis was performed by using the Microcal Origin 7.0 software for calculation of the enthalpy (ΔH). According to this, the DSC thermograms were fitted by the Gauss model, and the ΔH was calculated by integrating the area under the thermogram curve. Control measurements were carried out in the presence of DMSO at the same volumes used with the free curcumin/resveratrol.

■ ASSOCIATED CONTENT

Supporting Information

The Supporting Information is available free of charge at https://pubs.acs.org/doi/10.1021/acsapm.2c01316.

Description of the loading method of curcumin and resveratrol in dendrimers; drug loading graph of different curcumin/resveratrol ratios in dendrimers; cytochrome c oxidase activity graph; graphs of curcumin/resveratrol/dendrimer NPs affected mitochondria functionality in several biological assays (PDF)

■ AUTHOR INFORMATION

Corresponding Author

Raz Jelinek − *Department of Chemistry, Ben-Gurion University of the Negev, Beer Sheva 84105, Israel;* orcid.org/0000-0002-0336-1384; Email: razj@bgu.ac.il

Authors

Shani Ben-Zichri − *Department of Chemistry, Ben-Gurion University of the Negev, Beer Sheva 84105, Israel*

May Meltzer − *Avram and Stella Goldstein-Goren Department of Biotechnology Engineering and the National Institute of Biotechnology, Ben-Gurion University of the Negev, Beer Sheva 84105, Israel*

Shiran Lacham-Hartman − *Avram and Stella Goldstein-Goren Department of Biotechnology Engineering and the National Institute of Biotechnology, Ben-Gurion University of the Negev, Beer Sheva 84105, Israel*

Sofiya Kolusheva − *Ilze Katz Center for Nanotechnology, Ben-Gurion University, Beer Sheva 84105, Israel*

Uzi Hadad − *Ilze Katz Center for Nanotechnology, Ben-Gurion University, Beer Sheva 84105, Israel*

Niv Papo − *Avram and Stella Goldstein-Goren Department of Biotechnology Engineering and the National Institute of Biotechnology, Ben-Gurion University of the Negev, Beer Sheva 84105, Israel;* orcid.org/0000-0002-7056-2418

Complete contact information is available at: https://pubs.acs.org/10.1021/acsapm.2c01316

Funding

This research was partially funded by the Israel Science Foundation, Award no. 1657/20.

Notes

The authors declare no competing financial interest.

■ ACKNOWLEDGMENTS

We are grateful to Dr. Ran Taube for helping with the mitochondria isolation experiments.

■ ABBREVIATIONS:

NPs, nanoparticles; SH-SY5Y, neuroblastoma cells; CL, cardiolipin; DOPC, 1,2-dioleoyl-*sn*-glycero-3-phosphocholine; DMPC, 1,2-dimyristoyl-*sn*-glycero-3-phosphocholine; MLVs, multilamellar dispersions; GVs, giant vesicles; SMPs, submitochondrial particles; DSC, differential scanning calorimetry; COX, cytochrome c oxidase; TEM, transmission electron microscopy

■ REFERENCES

(1) Fadus, M. C.; Lau, C.; Bikhchandani, J.; Lynch, H. T. Curcumin: An age-old anti-inflammatory and anti-neoplastic agent. *J. Tradit Complement Med.* **2017**, *7*, 339−346.

(2) Rauf, A.; Imran, M.; Butt, M. S.; Nadeem, M.; Peters, D. G.; Mubarak, M. S. Resveratrol as an anti-cancer agent: A review. *Crit Rev. Food Sci. Nutr* **2018**, *58*, 1428−1447.

(3) Giordano, A.; Tommonaro, G. Curcumin and Cancer. *Nutrients* **2019**, *11*, 2376.

(4) Hu, S.; Xu, Y.; Meng, L.; Huang, L.; Sun, H. Curcumin inhibits proliferation and promotes apoptosis of breast cancer cells. *Exp Ther Med.* **2018**, *16*, 1266−1272.

(5) Zhou, S.; Zhang, S.; Shen, H.; Chen, W.; Xu, H.; Chen, X.; Sun, D.; Zhong, S.; Zhao, J.; Tang, J. Curcumin inhibits cancer progression through regulating expression of microRNAs. *Tumour Biol.* **2017**, *39*, 1010428317691680.

(6) Jiang, Z.; Chen, K.; Cheng, L.; Yan, B.; Qian, W.; Cao, J.; Li, J.; Wu, E.; Ma, Q.; Yang, W. Resveratrol and cancer treatment: updates. *Ann. N.Y. Acad. Sci.* **2017**, *1403*, 59−69.

(7) Vervandier-Fasseur, D.; Latruffe, N. The Potential Use of Resveratrol for Cancer Prevention. *Molecules* **2019**, *24*, 4506.

(8) Mortezaee, K.; Najafi, M.; Farhood, B.; Ahmadi, A.; Shabeeb, D.; Musa, A. E. Resveratrol as an Adjuvant for Normal Tissues Protection and Tumor Sensitization. *Curr. Cancer Drug Targets* **2020**, *20*, 130−145.

(9) Yu, C.; Yang, B.; Najafi, M. Targeting of cancer cell death mechanisms by curcumin: Implications to cancer therapy. *Basic Clin Pharmacol Toxicol* **2021**, *129*, 397−415.

(10) Fu, X.; He, Y.; Li, M.; Huang, Z.; Najafi, M. Targeting of the tumor microenvironment by curcumin. *Biofactors* **2021**, *47*, 914−932.

(11) Madreiter-Sokolowski, C. T.; Gottschalk, B.; Parichatikanond, W.; Eroglu, E.; Klec, C.; Waldeck-Weiermair, M.; Malli, R.; Graier, W. F. Resveratrol Specifically Kills Cancer Cells by a Devastating Increase in the Ca2+ Coupling Between the Greatly Tethered Endoplasmic Reticulum and Mitochondria. *Cell Physiol Biochem* **2016**, *39*, 1404−1420.
(12) Costa, P. S. D.; Ramos, P. S.; Ferreira, C.; Silva, J. L.; El-Bacha, T.; Fialho, E. Pro-Oxidant Effect of Resveratrol on Human Breast Cancer MCF-7 Cells is Associated with CK2 Inhibition. *Nutr Cancer* **2022**, *74*, 2142−2151.
(13) Kocyigit, A.; Guler, E. M. Curcumin induce DNA damage and apoptosis through generation of reactive oxygen species and reducing mitochondrial membrane potential in melanoma cancer cells. *Cell Mol. Biol. (Noisy-le-grand)* **2017**, *63*, 97−105.
(14) Ismail, N. I.; Othman, I.; Abas, F.; Lajis, N. H.; Naidu, R. Mechanism of Apoptosis Induced by Curcumin in Colorectal Cancer. *Int. J. Mol. Sci.* **2019**, *20*, 2454.
(15) Rodriguez-Enriquez, S.; Pacheco-Velazquez, S. C.; Marin-Hernandez, A.; Gallardo-Perez, J. C.; Robledo-Cadena, D. X.; Hernandez-Resendiz, I.; Garcia-Garcia, J. D.; Belmont-Diaz, J.; Lopez-Marure, R.; Hernandez-Esquivel, L.; Sanchez-Thomas, R.; Moreno-Sanchez, R. Resveratrol inhibits cancer cell proliferation by impairing oxidative phosphorylation and inducing oxidative stress. *Toxicol. Appl. Pharmacol.* **2019**, *370*, 65−77.
(16) Ashrafizadeh, M.; Javanmardi, S.; Moradi-Ozarlou, M.; Mohammadinejad, R.; Farkhondeh, T.; Samarghandian, S.; Garg, M. Natural products and phytochemical nanoformulations targeting mitochondria in oncotherapy: an updated review on resveratrol. *Biosci. Rep.* **2020**, *40* (4), No. BSR20200257.
(17) Singh, S.; Barnes, C. A.; D'Souza, J. S.; Hosur, R. V.; Mishra, P. Curcumin, a potential initiator of apoptosis via direct interactions with Bcl-xL and Bid. *Proteins* **2022**, *90*, 455−464.
(18) Patra, S.; Pradhan, B.; Nayak, R.; Behera, C.; Rout, L.; Jena, M.; Efferth, T.; Bhutia, S. K. Chemotherapeutic efficacy of curcumin and resveratrol against cancer: Chemoprevention, chemoprotection, drug synergism and clinical pharmacokinetics. *Semin Cancer Biol.* **2021**, *73*, 310−320.
(19) Zhou, X.; Afzal, S.; Zheng, Y. F.; Munch, G.; Li, C. G. Synergistic Protective Effect of Curcumin and Resveratrol against Oxidative Stress in Endothelial EAhy926 Cells. *Evidence-Based Complementary and Alternative Medicine* **2021**, *2021*, 2661025.
(20) Gumireddy, A.; Christman, R.; Kumari, D.; Tiwari, A.; North, E. J.; Chauhan, H. Preparation, Characterization, and In vitro Evaluation of Curcumin- and Resveratrol-Loaded Solid Lipid Nanoparticles. *AAPS PharmSciTech* **2019**, *20*, 145.
(21) Shindikar, A.; Singh, A.; Nobre, M.; Kirolikar, S. Curcumin and Resveratrol as Promising Natural Remedies with Nanomedicine Approach for the Effective Treatment of Triple Negative Breast Cancer. *J. Oncol* **2016**, *2016*, 9750785.
(22) Duan, Z.; Luo, Q.; Dai, X.; Li, X.; Gu, L.; Zhu, H.; Tian, X.; Zhang, H.; Gong, Q.; Gu, Z.; Luo, K. Synergistic Therapy of a Naturally Inspired Glycopolymer-Based Biomimetic Nanomedicine Harnessing Tumor Genomic Instability. *Adv. Mater.* **2021**, *33*, No. 2104594.
(23) Li, J.; Liang, H.; Liu, J.; Wang, Z. Poly (amidoamine) (PAMAM) dendrimer mediated delivery of drug and pDNA/siRNA for cancer therapy. *Int. J. Pharm.* **2018**, *546*, 215−225.
(24) Palmerston Mendes, L.; Pan, J.; Torchilin, V. P. Dendrimers as Nanocarriers for Nucleic Acid and Drug Delivery in Cancer Therapy. *Molecules* **2017**, *22*, 1401.
(25) Sharma, A. K.; Gothwal, A.; Kesharwani, P.; Alsaab, H.; Iyer, A. K.; Gupta, U. Dendrimer nanoarchitectures for cancer diagnosis and anticancer drug delivery. *Drug Discov Today* **2017**, *22*, 314−326.
(26) Abedi-Gaballu, F.; Dehghan, G.; Ghaffari, M.; Yekta, R.; Abbaspour-Ravasjani, S.; Baradaran, B.; Dolatabadi, J. E. N.; Hamblin, M. R. PAMAM dendrimers as efficient drug and gene delivery nanosystems for cancer therapy. *Appl. Mater. Today* **2018**, *12*, 177−190.
(27) Dubey, S. K.; Salunkhe, S.; Agrawal, M.; Kali, M.; Singhvi, G.; Tiwari, S.; Saraf, S.; Saraf, S.; Alexander, A. Understanding the Pharmaceutical Aspects of Dendrimers for the Delivery of Anticancer Drugs. *Curr. Drug Targets* **2020**, *21*, 528−540.
(28) Svenson, S.; Tomalia, D. A. Dendrimers in biomedical applications−reflections on the field. *Adv. Drug Deliv Rev.* **2005**, *57*, 2106−2129.
(29) Cui, Y.; Liang, B.; Wang, L.; Zhu, L.; Kang, J.; Sun, H.; Chen, S. Enhanced biocompatibility of PAMAM dendrimers benefiting from tuning their surface charges. *Mater. Sci. Eng. C Mater. Biol. Appl.* **2018**, *93*, 332−340.
(30) Hu, H.; Wang, H.; Liang, S.; Li, X.; Wang, D. Synthesis and characterization of a PAMAM dendrimer nanocarrier functionalized by HA for targeted gene delivery systems and evaluation in vitro. *J. Biomater Sci. Polym. Ed* **2021**, *32*, 205−228.
(31) Mekuria, S. L.; Li, J.; Song, C.; Gao, Y.; Ouyang, Z.; Shen, M.; Shi, X. Facile Formation of PAMAM Dendrimer Nanoclusters for Enhanced Gene Delivery and Cancer Gene Therapy. *ACS Appl. Bio Mater.* **2021**, *4*, 7168−7175.
(32) Kheraldine, H.; Rachid, O.; Habib, A. M.; Al Moustafa, A. E.; Benter, I. F.; Akhtar, S. Emerging innate biological properties of nano-drug delivery systems: A focus on PAMAM dendrimers and their clinical potential. *Adv. Drug Deliv Rev.* **2021**, *178*, 113908.
(33) Thanh, V. M.; Nguyen, T. H.; Tran, T. V.; Ngoc, U. P.; Ho, M. N.; Nguyen, T. T.; Chau, Y. N. T.; Le, V. T.; Tran, N. Q.; Nguyen, C. K.; Nguyen, D. H. Low systemic toxicity nanocarriers fabricated from heparin-mPEG and PAMAM dendrimers for controlled drug release. *Mater. Sci. Eng. C Mater. Biol. Appl.* **2018**, *82*, 291−298.
(34) Domanska, U.; Zolek-Tryznowska, Z. Thermodynamic properties of hyperbranched polymer, Boltorn U3000, using inverse gas chromatography. *J. Phys. Chem. B* **2009**, *113*, 15312−15321.
(35) Reul, R.; Renette, T.; Bege, N.; Kissel, T. Nanoparticles for paclitaxel delivery: a comparative study of different types of dendritic polyesters and their degradation behavior. *Int. J. Pharm.* **2011**, *407*, 190−196.
(36) Zhao, C.; Wang, N.; Wang, L.; Huang, H.; Zhang, R.; Yang, F.; Xie, Y.; Ji, S.; Li, J. R. Hybrid membranes of metal-organic molecule nanocages for aromatic/aliphatic hydrocarbon separation by pervaporation. *Chem. Commun. (Camb)* **2014**, *50*, 13921−13923.
(37) Sala, M.; Locher, F.; Bonvallet, M.; Agusti, G.; Elaissari, A.; Fessi, H. Diclofenac Loaded Lipid Nanovesicles Prepared by Double Solvent Displacement for Skin Drug Delivery. *Pharm. Res.* **2017**, *34*, 1908−1924.
(38) Lu, Z.; Schaarsberg, M. H. K.; Zhu, X.; Yeo, L. Y.; Lohse, D.; Zhang, X. Universal nanodroplet branches from confining the Ouzo effect. *Proc. Natl. Acad. Sci. U. S. A.* **2017**, *114*, 10332−10337.
(39) Subia, B.; Kundu, S. C. Drug loading and release on tumor cells using silk fibroin-albumin nanoparticles as carriers. *Nanotechnology* **2013**, *24*, 035103.
(40) Carlmark, A.; Malmstrom, E.; Malkoch, M. Dendritic architectures based on bis-MPA: functional polymeric scaffolds for application-driven research. *Chem. Soc. Rev.* **2013**, *42*, 5858−5879.
(41) Mondal, S.; Dorozhkin, S. V.; Pal, U. Recent progress on fabrication and drug delivery applications of nanostructured hydroxyapatite. *Wiley Interdiscip Rev. Nanomed Nanobiotechnol* **2018**, *10*, No. e1504.
(42) Figueiras, T. S.; Neves-Petersen, M. T.; Petersen, S. B. Activation energy of light induced isomerization of resveratrol. *J. Fluoresc* **2011**, *21*, 1897−1906.
(43) Karimi, M.; Mashreghi, M.; Shokooh Saremi, S.; Jaafari, M. R. Spectrofluorometric Method Development and Validation for the Determination of Curcumin in Nanoliposomes and Plasma. *J. Fluoresc* **2020**, *30*, 1113−1119.
(44) Kosovic, E.; Topiar, M.; Curinova, P.; Sajfrtova, M. Stability testing of resveratrol and viniferin obtained from Vitis vinifera L. by various extraction methods considering the industrial viewpoint. *Sci. Rep* **2020**, *10*, 5564.
(45) Ma, Y.; Chen, S.; Liao, W.; Zhang, L.; Liu, J.; Gao, Y. Formation, Physicochemical Stability, and Redispersibility of

https://doi.org/10.1021/acsapm.2c01316
ACS Appl. Polym. Mater. XXXX, XXX, XXX−XXX

Curcumin-Loaded Rhamnolipid Nanoparticles Using the pH-Driven Method. *J. Agric. Food Chem.* **2020**, *68*, 7103−7111.
(46) Yu, M.; Yuan, W.; Li, D.; Schwendeman, A.; Schwendeman, S. P. Predicting drug release kinetics from nanocarriers inside dialysis bags. *J. Controlled Release* **2019**, *315*, 23−30.
(47) Peppicelli, S.; Andreucci, E.; Ruzzolini, J.; Laurenzana, A.; Margheri, F.; Fibbi, G.; Del Rosso, M.; Bianchini, F.; Calorini, L. The acidic microenvironment as a possible niche of dormant tumor cells. *Cell. Mol. Life Sci.* **2017**, *74*, 2761−2771.
(48) Thews, O.; Riemann, A. Tumor pH and metastasis: a malignant process beyond hypoxia. *Cancer Metastasis Rev.* **2019**, *38*, 113−129.
(49) Asgharzadeh, M. R.; Barar, J.; Pourseif, M. M.; Eskandani, M.; Jafari Niya, M.; Mashayekhi, M. R.; Omidi, Y. Molecular machineries of pH dysregulation in tumor microenvironment: potential targets for cancer therapy. *Bioimpacts* **2017**, *7*, 115−133.
(50) Mogharbel, B. F.; Francisco, J. C.; Irioda, A. C.; Dziedzic, D. S. M.; Ferreira, P. E.; de Souza, D.; de Souza, C.; Neto, N. B.; Guarita-Souza, L. C.; Franco, C. R. C.; Nakamura, C. V.; Kaplum, V.; Mazzarino, L.; Lemos-Senna, E.; Borsali, R.; Soto, P. A.; Setton-Avruj, P.; Abdelwahid, E.; de Carvalho, K. A. T.; et al. Fluorescence properties of curcumin-loaded nanoparticles for cell tracking. *Int. J. Nanomedicine* **2018**, *13*, 5823−5836.
(51) Sahin, M.; Oncu, G.; Yilmaz, M. A.; Ozkan, D.; Saybasili, H. Transformation of SH-SY5Y cell line into neuron-like cells: Investigation of electrophysiological and biomechanical changes. *Neurosci. Lett.* **2021**, *745*, 135628.
(52) Sanidad, K. Z.; Sukamtoh, E.; Xiao, H.; McClements, D. J.; Zhang, G. Curcumin: Recent Advances in the Development of Strategies to Improve Oral Bioavailability. *Annu. Rev. Food Sci. Technol.* **2019**, *10*, 597−617.
(53) Ternullo, S.; Gagnat, E.; Julin, K.; Johannessen, M.; Basnet, P.; Vanic, Z.; Skalko-Basnet, N. Liposomes augment biological benefits of curcumin for multitargeted skin therapy. *Eur. J. Pharm. Biopharm* **2019**, *144*, 154−164.
(54) Fu, X.; Li, M.; Tang, C.; Huang, Z.; Najafi, M. Targeting of cancer cell death mechanisms by resveratrol: a review. *Apoptosis* **2021**, *26*, 561−573.
(55) Kabir, M. T.; Rahman, M. H.; Akter, R.; Behl, T.; Kaushik, D.; Mittal, V.; Pandey, P.; Akhtar, M. F.; Saleem, A.; Albadrani, G. M.; Kamel, M.; Khalifa, S. A. M.; El-Seedi, H. R.; Abdel-Daim, M. M. Potential Role of Curcumin and Its Nanoformulations to Treat Various Types of Cancers. *Biomolecules* **2021**, *11*, 392.
(56) Aparicio-Trejo, O. E.; Tapia, E.; Molina-Jijon, E.; Medina-Campos, O. N.; Macias-Ruvalcaba, N. A.; Leon-Contreras, J. C.; Hernandez-Pando, R.; Garcia-Arroyo, F. E.; Cristobal, M.; Sanchez-Lozada, L. G.; Pedraza-Chaverri, J. Curcumin prevents mitochondrial dynamics disturbances in early 5/6 nephrectomy: Relation to oxidative stress and mitochondrial bioenergetics. *Biofactors* **2017**, *43*, 293−310.
(57) Mortezaee, K.; Salehi, E.; Mirtavoos-Mahyari, H.; Motevaseli, E.; Najafi, M.; Farhood, B.; Rosengren, R. J.; Sahebkar, A. Mechanisms of apoptosis modulation by curcumin: Implications for cancer therapy. *J. Cell Physiol* **2019**, *234*, 12537−12550.
(58) Repossi, G.; Das, U. N.; Eynard, A. R. Molecular Basis of the Beneficial Actions of Resveratrol. *Arch Med. Res.* **2020**, *51*, 105−114.
(59) Takashina, M.; Inoue, S.; Tomihara, K.; Tomita, K.; Hattori, K.; Zhao, Q. L.; Suzuki, T.; Noguchi, M.; Ohashi, W.; Hattori, Y. Different effect of resveratrol to induction of apoptosis depending on the type of human cancer cells. *Int. J. Oncol.* **2017**, *50*, 787−797.
(60) Finkel, T.; Menazza, S.; Holmstrom, K. M.; Parks, R. J.; Liu, J.; Sun, J.; Liu, J.; Pan, X.; Murphy, E. The ins and outs of mitochondrial calcium. *Circ. Res.* **2015**, *116*, 1810−1819.
(61) Vakifahmetoglu-Norberg, H.; Ouchida, A. T.; Norberg, E. The role of mitochondria in metabolism and cell death. *Biochem. Biophys. Res. Commun.* **2017**, *482*, 426−431.
(62) Danese, A.; Patergnani, S.; Bonora, M.; Wieckowski, M. R.; Previati, M.; Giorgi, C.; Pinton, P. Calcium regulates cell death in cancer: Roles of the mitochondria and mitochondria-associated membranes (MAMs). *Biochim Biophys Acta Bioenerg* **2017**, *1858*, 615−627.
(63) Srinivasan, S.; Guha, M.; Kashina, A.; Avadhani, N. G. Mitochondrial dysfunction and mitochondrial dynamics-The cancer connection. *Biochim Biophys Acta Bioenerg* **2017**, *1858*, 602−614.
(64) Peterson, J. A.; Crowther, C. M.; Andrus, M. B.; Kenealey, J. D. Resveratrol derivatives increase cytosolic calcium by inhibiting plasma membrane ATPase and inducing calcium release from the endoplasmic reticulum in prostate cancer cells. *Biochem Biophys Rep* **2019**, *19*, 100667.
(65) Zheng, P.; Ding, B.; Shi, R.; Jiang, Z.; Xu, W.; Li, G.; Ding, J.; Chen, X. A Multichannel Ca(2+) Nanomodulator for Multilevel Mitochondrial Destruction-Mediated Cancer Therapy. *Adv. Mater.* **2021**, *33*, No. 2007426.
(66) Timon-Gomez, A.; Nyvltova, E.; Abriata, L. A.; Vila, A. J.; Hosler, J.; Barrientos, A. Mitochondrial cytochrome c oxidase biogenesis: Recent developments. *Semin Cell Dev Biol.* **2018**, *76*, 163−178.
(67) Riles, W. L.; Erickson, J.; Nayyar, S.; Atten, M. J.; Attar, B. M.; Holian, O. Resveratrol engages selective apoptotic signals in gastric adenocarcinoma cells. *World J. Gastroenterol* **2006**, *12*, 5628−5634.
(68) Sharma, S.; Zhuang, Y.; Ying, Z.; Wu, A.; Gomez-Pinilla, F. Dietary curcumin supplementation counteracts reduction in levels of molecules involved in energy homeostasis after brain trauma. *Neuroscience* **2009**, *161*, 1037−1044.
(69) Kalashnikov, D. S.; Grivennikova, V. G.; Vinogradov, A. D. Submitochondrial fragments of brain mitochondria: general characteristics and catalytic properties of NADH:ubiquinone oxidoreductase (complex I). *Biochemistry (Mosc)* **2011**, *76*, 209−216.
(70) Zorova, L. D.; Popkov, V. A.; Plotnikov, E. Y.; Silachev, D. N.; Pevzner, I. B.; Jankauskas, S. S.; Babenko, V. A.; Zorov, S. D.; Balakireva, A. V.; Juhaszova, M.; Sollott, S. J.; Zorov, D. B. Mitochondrial membrane potential. *Anal. Biochem.* **2018**, *552*, 50−59.
(71) Banfalvi, G. Methods to detect apoptotic cell death. *Apoptosis* **2017**, *22*, 306−323.
(72) Fantini, M.; Benvenuto, M.; Masuelli, L.; Frajese, G. V.; Tresoldi, I.; Modesti, A.; Bei, R. In vitro and in vivo antitumoral effects of combinations of polyphenols, or polyphenols and anticancer drugs: perspectives on cancer treatment. *Int. J. Mol. Sci.* **2015**, *16*, 9236−9282.
(73) Malhotra, A.; Nair, P.; Dhawan, D. K. Study to evaluate molecular mechanics behind synergistic chemo-preventive effects of curcumin and resveratrol during lung carcinogenesis. *PLoS One* **2014**, *9*, No. e93820.
(74) Du, Q.; Hu, B.; An, H. M.; Shen, K. P.; Xu, L.; Deng, S.; Wei, M. M. Synergistic anticancer effects of curcumin and resveratrol in Hepa1−6 hepatocellular carcinoma cells. *Oncol. Rep.* **2013**, *29*, 1851−1858.
(75) Shakibaei, M.; Mobasheri, A.; Buhrmann, C. Curcumin synergizes with resveratrol to stimulate the MAPK signaling pathway in human articular chondrocytes in vitro. *Genes Nutr* **2011**, *6*, 171−179.
(76) Majumdar, A. P.; Banerjee, S.; Nautiyal, J.; Patel, B. B.; Patel, V.; Du, J.; Yu, Y.; Elliott, A. A.; Levi, E.; Sarkar, F. H. Curcumin synergizes with resveratrol to inhibit colon cancer. *Nutr Cancer* **2009**, *61*, 544−553.
(77) Reis, A.; Perez-Gregorio, R.; Mateus, N.; de Freitas, V. Interactions of dietary polyphenols with epithelial lipids: advances from membrane and cell models in the study of polyphenol absorption, transport and delivery to the epithelium. *Crit Rev. Food Sci. Nutr* **2021**, *61*, 3007−3030.
(78) Ben-Zichri, S.; Kolusheva, S.; Danilenko, M.; Ossikbayeva, S.; Stabbert, W. J.; Poggio, J. L.; Stein, D. E.; Orynbayeva, Z.; Jelinek, R. Cardiolipin mediates curcumin interactions with mitochondrial membranes. *Biochim Biophys Acta Biomembr* **2019**, *1861*, 75−82.
(79) Toyota, T.; Zhang, Y. Identifying and Manipulating Giant Vesicles: Review of Recent Approaches. *Micromachines (Basel)* **2022**, *13*, 644.

https://doi.org/10.1021/acsapm.2c01316
ACS Appl. Polym. Mater. XXXX, XXX, XXX−XXX

(80) Chountoulesi, M.; Naziris, N.; Mavromoustakos, T.; Demetzos, C. A Differential Scanning Calorimetry (DSC) Experimental Protocol for Evaluating the Modified Thermotropic Behavior of Liposomes with Incorporated Guest Molecules. *Methods Mol. Biol.* **2021**, *2207*, 299−312.
(81) Berretta, M.; Bignucolo, A.; Di Francia, R.; Comello, F.; Facchini, G.; Ceccarelli, M.; Iaffaioli, R. V.; Quagliariello, V.; Maurea, N. Resveratrol in Cancer Patients: From Bench to Bedside. *Int. J. Mol. Sci.* **2020**, *21*, 2945.
(82) Duda, M.; Cygan, K.; Wisniewska-Becker, A. Effects of Curcumin on Lipid Membranes: an EPR Spin-label Study. *Cell Biochem Biophys* **2020**, *78*, 139−147.
(83) Hassanalilou, T.; Ghavamzadeh, S.; Khalili, L. Curcumin and Gastric Cancer: a Review on Mechanisms of Action. *J. Gastrointest Cancer* **2019**, *50*, 185−192.
(84) Kim, S. E.; Shin, S. H.; Lee, J. Y.; Kim, C. H.; Chung, I. K.; Kang, H. M.; Park, H. R.; Park, B. S.; Kim, I. R. Resveratrol Induces Mitochondrial Apoptosis and Inhibits Epithelial-Mesenchymal Transition in Oral Squamous Cell Carcinoma Cells. *Nutr Cancer* **2018**, *70*, 125−135.
(85) Pricci, M.; Girardi, B.; Giorgio, F.; Losurdo, G.; Ierardi, E.; Di Leo, A. Curcumin and Colorectal Cancer: From Basic to Clinical Evidences. *Int. J. Mol. Sci.* **2020**, *21*, 2364.
(86) Bauer, T. M.; Murphy, E. Role of Mitochondrial Calcium and the Permeability Transition Pore in Regulating Cell Death. *Circ. Res.* **2020**, *126*, 280−293.
(87) Martinez Rivas, C. J.; Tarhini, M.; Badri, W.; Miladi, K.; Greige-Gerges, H.; Nazari, Q. A.; Galindo Rodriguez, S. A.; Roman, R. A.; Fessi, H.; Elaissari, A. Nanoprecipitation process: From encapsulation to drug delivery. *Int. J. Pharm.* **2017**, *532*, 66−81.
(88) Zichri, S. B.; Kolusheva, S.; Shames, A. I.; Schneiderman, E. A.; Poggio, J. L.; Stein, D. E.; Doubijensky, E.; Levy, D.; Orynbayeva, Z.; Jelinek, R. Mitochondria membrane transformations in colon and prostate cancer and their biological implications. *Biochim Biophys Acta Biomembr* **2021**, *1863*, 183471.
(89) Lampl, T.; Crum, J. A.; Davis, T. A.; Milligan, C.; Del Gaizo Moore, V. Isolation and functional analysis of mitochondria from cultured cells and mouse tissue. *J. Visualized Exp.* **2015**, *97*, 52076.
(90) Murai, M.; Miyoshi, H. Photoaffinity Labeling of Respiratory Complex I in Bovine Heart Submitochondrial Particles by Photoreactive [(125)I] amilorides. *Bio Protoc* **2019**, *9*, No. e3349.
(91) Walde, P.; Cosentino, K.; Engel, H.; Stano, P. Giant vesicles: preparations and applications. *Chembiochem* **2010**, *11*, 848−865.
(92) Park, E. K.; Kim, S. Y.; Lee, S. B.; Lee, Y. M. Folate-conjugated methoxy poly(ethylene glycol)/poly(epsilon-caprolactone) amphiphilic block copolymeric micelles for tumor-targeted drug delivery. *J. Controlled Release* **2005**, *109*, 158−168.
(93) Kopcova, K.; Mikulova, L.; Pechova, I.; Sztachova, T.; Cizmar, E.; Jancura, D.; Fabian, M. Modulation of the electron-proton coupling at cytochrome a by the ligation of the oxidized catalytic center in bovine cytochrome c oxidase. *Biochim Biophys Acta Bioenerg* **2020**, *1861*, 148237.

https://doi.org/10.1021/acsapm.2c01316
ACS Appl. Polym. Mater. XXXX, XXX, XXX−XXX